Instrument Science Report COS 2017-17

Focusing the COS/FUV G160M and G140L Gratings at Lifetime Position 4

Andrew Fox[1], Steven Penton[1], Jo Taylor[1]

[1] Space Telescope Science Institute, 3700 San Martin Drive, Baltimore, MD 21218

August 28, 2017

ABSTRACT

In December 2016 focus sweeps were performed at the fourth lifetime position (LP4) of the COS/FUV detector with the G160M and G140L gratings. In this ISR we present the results. The focus sweeps involved observations of the stars Feige 48 and AzV75 at a range of focus settings. An auto-correlation technique was used to find the minimal line widths of absorption lines and therefore find the optimal focus setting. This process yielded focus offsets relative to the LP3 foci of +262 for G160M/1600, and +260 for G140L/1105. A comparison with ray-trace models shows that the G140L/1105 focus offset is within expectations when errors are considered, and the G160M/1600 focus differs from expectations at the 2.5σ level. The derived focus offsets were updated in the flight software tables in February 2017 and will be used for routine LP4 operations.

Contents

1. Introduction

When moving the COS FUV detector to a new lifetime position, off-axis optical effects degrade the spectral focus. To correct for this, focus sweep programs are executed to determine the optimal focus values at the new position, and these values are uploaded into the flight software. These programs are conducted separately for each grating since the focus position is grating- and wavelength-dependent. In December 2016, the G160M and G140L gratings were focused at LP4 under Program 14874, in preparation for the move to LP4 expected for October 2017. This ISR presents the results from that program. LP4 is located $-5.0''$ in the cross-dispersion direction from LP1 (LP3 is at -2.5"). Similar analyses at LP1 are described by Lennon et al. (2010) and Ghavamian et al. (2012), at LP2 by Oliveira et al. (2013), and at LP3 by Fox et al. (2015).

The G130M/1222 and G130M/1309 settings at LP4 were focused in a separate program and are described in a separate report (Sonnentrucker et al. 2017). This separation occurred because the G130M sweeps were conducted in an earlier phase of the LP4 preparations (the exploratory phase) whereas the G160M and G140L sweeps were conducted at a later stage (the enabling phase). Final focus values from both programs are presented together in Table 4 of this ISR.

The basic principle of a focus sweep is to observe a star at a number of focus positions, and then use a spectral line-width analysis to determine which position yields the sharpest photospheric and interstellar absorption lines (i.e, the spectra best in focus). This process can be repeated for different gratings and central wavelengths (cenwaves). For each grating/cenwave combination, a focus offset is determined relative to the current value encoded in the flight software. The derived focus offsets can be compared with the predictions of ray-trace models, to assess whether they are in agreement with expectations. Once the final focus values for each setting are determined, they are specified in the flight software tables for use in subsequent LP4 observations.

Following Lennon et al. (2010), we assume that the *relative* focus offset determined for a given grating/cenwave combination is applicable to all cenwaves of that grating, except for the G130M blue modes, which we treat as separate cases since the blue cenwaves (G130M/1055, 1096, and 1222) are known to have different foci than the other G130M cenwaves (1291, 1300, 1309, 1318, and 1327). However, the *absolute* focus values vary from cenwave to cenwave.

2. Ray-Trace Models

Ray-trace (RT) models predict how the focus of the COS FUV instrument (measured by the width of resolved absorption lines) depends on commanded focus position and on wavelength. We produced a set of models using a modified version of Eric Wilkinson's IDL Interactive Ray-Trace (IRT) routine (Version 2.8, Parsec Technology, 1989, Webster Cash). IRT is a geometric ray-trace code used to determine the original COS optical design. The code models the dispersion line spread function (LSF) and the cross-

dispersion LSF to generate the RT prediction. The code has been modified to account for the effects of grating rotation, multiple central wavelengths, and aperture/pointing offsets. The models were computed for the LP4 position, which is located at $-5.0''$ in the cross-dispersion direction relative to LP1 with no offset in the dispersion direction.

The focus curves predicted from these RT models are shown in Figure 1 for the G160M/1600 and G140L/1105 settings, in the form of line width (FWHM) vs focus-step offset Δf relative to the LP3 position. The predictions are wavelength-dependent, with a functional form that can be well described by cubic polynomials. For each grating, we average the minima derived from the ten wavelengths to find the overall minimum for that grating/cenwave combination.

3. Observations

The LP4 focus-sweep involved COS/FUV observations of two bright stars (Feige 48 and AzV75) for a total of five orbits spread over two visits. Feige 48 was observed with the G160M/1600 setting, and AzV75 was observed with the G140L/1105 setting. Feige 48 is an sdB star with a low projected rotational velocity and many narrow photospheric absorption lines (widths $<5\,\mathrm{km\,s^{-1}}$) in the UV, rendering it an ideal target for this focus sweep, which relies on a line-width analysis. AzV75 (an O5.5 supergiant star in the SMC) was used for the G140L focus sweep since Feige 48 is too bright for that grating.

The data were obtained in December 2016; see Tables 1 and 2 for observational details of each exposure. The sweeps moved from commanded focus positions of -800 to +1000 in increments of 200 (10.4 microns). In addition, for the G140L/1105 sweep a finer step size of 100 was used between positions of -200 and $+200$, in order to better sample the focus curve near the central minimum, and an additional exposure at a commanded offset of zero was included at the end of the sweep. This was because a small amount of time was left at the end of the orbit, enabling an extra exposure, again at offset zero but with a different breathing correction.

The data were reduced manually using `calcos`, since LP4 observations were not supported by the automatic pipeline at the time these observations were taken. The focus analysis used the extracted 1D spectra (`x1d` files).

Before finding the minima of the focus curves, a correction must be made for thermal breathing of the telescope. Breathing causes the actual focus position at a given time to differ from the commanded focus position. Based on temperatures measured by sensors on board *HST*, a breathing model can be used to determine the breathing correction. This model is known as the *HST* focus model tool[1], which computes the focus offset (in microns) with respect to the nominal value at the time of observation. The *HST* focus is derived from WFC3/UVIS1 data, and is assumed to apply to COS. We used this tool to determine the breathing-corrected focus offset at the start of each exposure in the program, as shown in Figure 2. The focus offsets in microns are multiplied by a factor of 19.2 (see Oliveira et al. 2013) to give the breathing correction in

[1] http://focustool.stsci.edu/cgi-bin/control.py

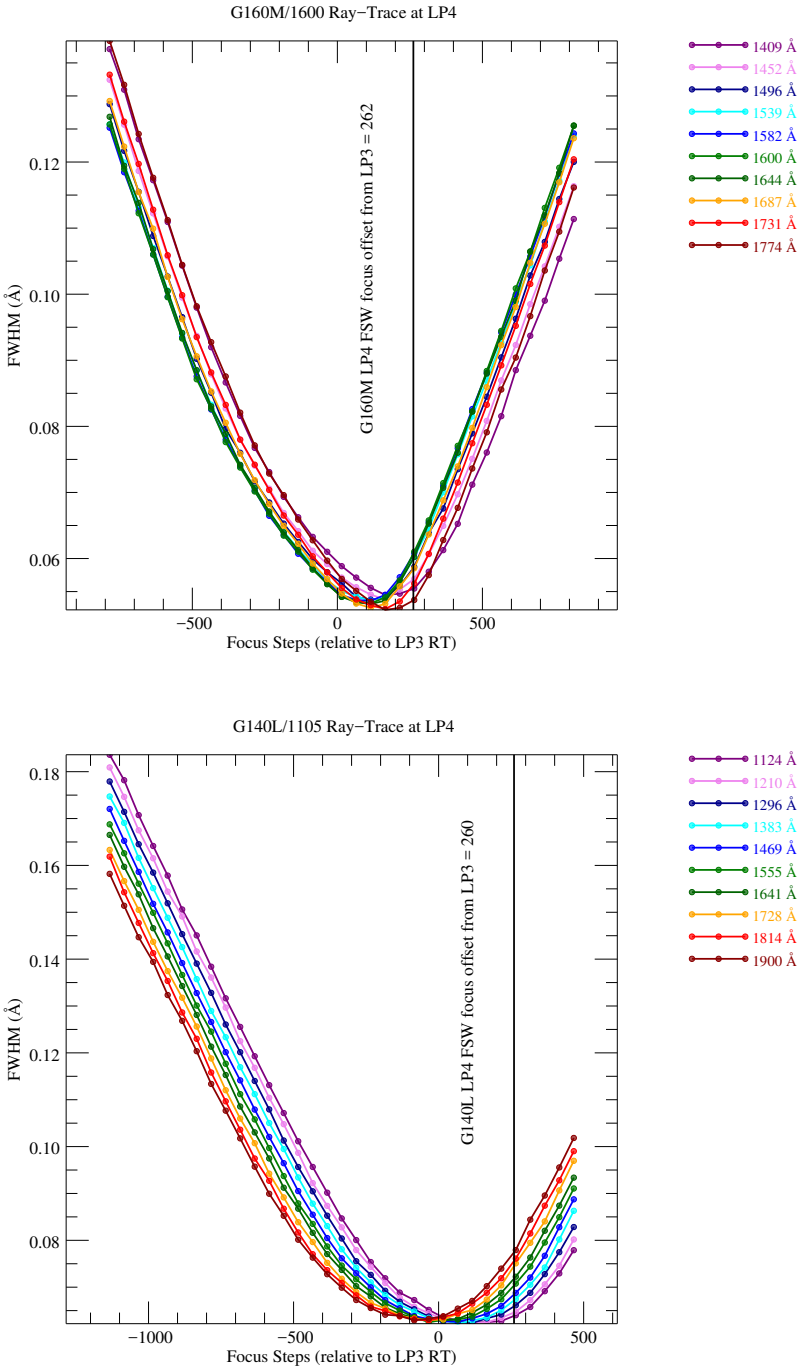

Figure 1. Focus curves at LP4 generated by RT models for the G160M/1600 (top) and G140L/1105 (bottom) settings. Absorption-line width (FWHM) is plotted against focus offset relative to LP3 for various wavelengths (colored lines). The best-fit offsets derived in this ISR are shown with the vertical solid lines. Differences between the RT models and derived focus position are discussed in Section 5.

Table 1. Log of exposures and focus offsets for G160M/1600 sweep at LP4.

Filename	Segment	Start Time (UT)	Commanded Focus Offset	Breathing-corrected Focus Offset
lddf01rvs	FUVA&FUVB	12/13/16 20:19	−800	−797
lddf01rxq	FUVA&FUVB	12/13/16 20:32	−600	−568
lddf01rzq	FUVA&FUVB	12/13/16 20:45	−400	−383
lddf01s3q	FUVA&FUVB	12/13/16 21:40	−200	−226
lddf01s5q	FUVA&FUVB	12/13/16 21:55	0	19
lddf01s7q	FUVA&FUVB	12/13/16 22:10	200	237
lddf01s9q	FUVA&FUVB	12/13/16 23:17	400	387
lddf01sbq	FUVA&FUVB	12/13/16 23:29	600	627
lddf01sdq	FUVA&FUVB	12/13/16 23:42	800	847
lddf01sfq	FUVA&FUVB	12/13/16 23:54	1000	1043

Table 2. Log of exposures and focus offsets for the G140L/1105 sweep at LP4. Only detector segment FUVA was used following standard practice for this CENWAVE.

Filename	Segment	Start Time (UT)	Commanded Focus Offset	Breathing-corrected Focus Offset
lddf02tkq	FUVA	12/22/2016 11:32	−800	−918
lddf02tmq	FUVA	12/22/2016 11:39	−600	−678
lddf02toq	FUVA	12/22/2016 11:45	−400	−468
lddf02tqq	FUVA	12/22/2016 11:52	−200	−260
lddf02tsq	FUVA	12/22/2016 11:58	−100	−156
lddf02tuq	FUVA	12/22/2016 12:05	0	−48
lddf02twq	FUVA	12/22/2016 12:11	100	70
lddf02tyq	FUVA	12/22/2016 12:18	200	177
lddf02u0q	FUVA	12/22/2016 13:05	400	354
lddf02u2q	FUVA	12/22/2016 13:11	600	502
lddf02u4q	FUVA	12/22/2016 13:18	800	687
lddf02u6q	FUVA	12/22/2016 13:24	1000	878
lddf02u8q	FUVA	12/22/2016 13:31	0	−106

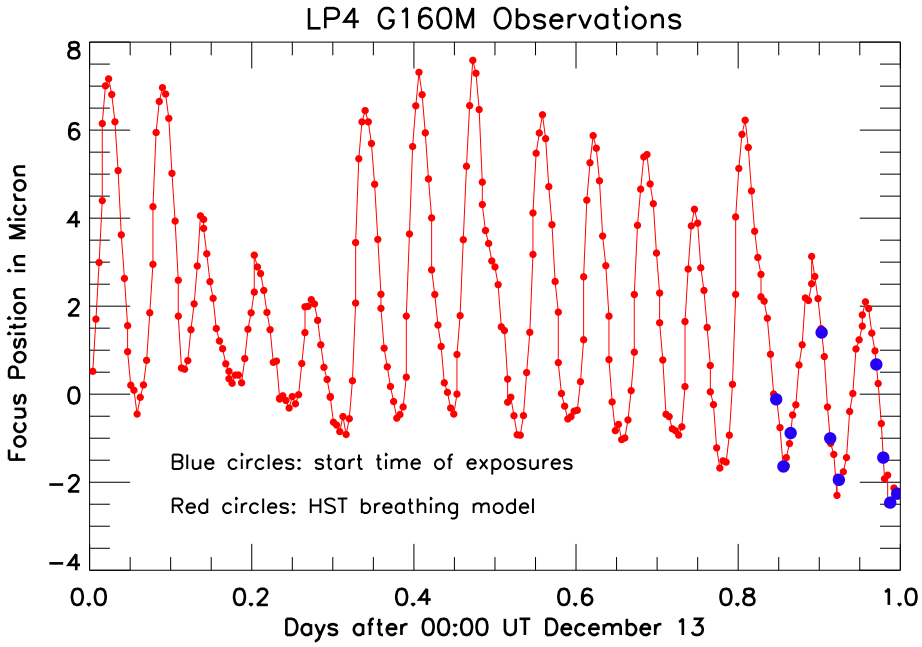

Figure 2. *HST* breathing model (red line) for WFC3/UVIS1 (applicable to COS) during the time when the G160M observations were taken. The curve shows the focus position in microns as a function of time. Each cycle has a period of one HST orbit and reflects the thermal breathing of the telescope. Blue points indicate the times when each exposure in the focus sweep began. The breathing correction applied to each commanded focus offset is directly proportional to the focus position at the time of observation.

units of COS/OSM1 focus steps. The sense of the offset is such that the corrected value is given by:

breathing-corrected focus offset = commanded focus offset–breathing correction.

4. Data Analysis

Following earlier COS/FUV focus sweeps, we use an auto-correlation method to determine the best-fit focus in each setting. In this method, broad regions of FUV spectra containing narrow absorption lines are selected and cross-correlated with themselves. Photospheric lines are used with Feige 48 and interstellar lines with AZV75. In the Feige 48 analysis, regions are chosen to be free from strong interstellar absorption lines. Airglow emission (Lyα and O I 1302) regions are avoided in the analysis of both targets. The wavelength regions used are given in Table 3. The regions are similar to those used in the LP1, LP2, and LP3 focus sweeps, although with modifications to select wavelength ranges as broad as possible without contamination from ISM absorption and/or

Table 3. Wavelength ranges $\delta\lambda_n$ used for auto-correlation analysis, and corresponding focus offsets (Δf_n) derived in each range. The ranges were selected to be free from strong interstellar absorption lines in the G160M analysis and free of geocoronal airglow emission in both the G160M and G140L analysis.

Setting	$\delta\lambda_1$ (Å)	Δf_1	$\delta\lambda_2$ (Å)	Δf_2	$\delta\lambda_3$ (Å)	Δf_3
G160M/1600/FUVA	1612–1666	+309	1673–1768	+248	...	...
G160M/1600/FUVB	1413–1524	+276	1528–1578	+350	...	...
G140L/1105/FUVA	1245–1280	+235	1310–1500	+235	1600–1900	+241

airglow emission.

The width of the auto-correlation function (ACF) provides a statistical measure of the widths of the absorption lines contained within the spectral region, and hence of the spectral resolution and the focus: the better focused the instrument, the narrower the absorption lines, and the narrower the width of the ACF. For each mode observed, and for each position in the focus sweep, we calculate the ACF, normalize it to unity at its peak, and fit it with a Gaussian function to determine its width.

We then construct curves of ACF width vs corrected focus offset (hereafter, focus curves), and fit these curves with cubic functions to determine their minima. Cubic functions provide a good representation of the G160M focus curve, but are less successful in reproducing the G140L curve, which shows an asymmetric shape with a shallow minimum (this was true for G140L at earlier lifetime positions too; Oliveira et al. 2013, Fox et al. 2015). Since the ACF technique samples the focus curve over a range in wavelength, we are effectively optimizing resolution for the average wavelength within the spectral windows. The focus curves derived in this manner are shown in Figures 3 and 4, with the best-fit focus offset (defined as the focus offset where the ACF is minimized) annotated on the panel. We also measure the full-width at half-maximum (FWHM) of the ACF as an alternative measure of its line width, and verify for each mode that the focus curves show similar minima when using the FWHM as when using the Gaussian width, but we adopt the Gaussian width in our final analysis following the strategy used in the LP3 focus sweep (Fox et al. 2015).

As a check on the validity of our ACF technique, we selected regions of the spectra in each focus sweep that contain strong metal absorption lines (either photospheric or interstellar), and conducted visual inspections of these regions at each focus position, to determine if the best-fit focus showed the sharpest lines. This exercise is illustrated in the appendix, with one figure for each grating/cenwave setting (Figures 5 and 6). For example, for G160M/1600 the best-fit focus offset found from the ACF technique is +232 and there is an exposure in the sweep at a (corrected) focus position of +237, so one expects (and indeed finds) that the spectra from that exposure are sharper than those obtained at the preceding or following step in the sweep.

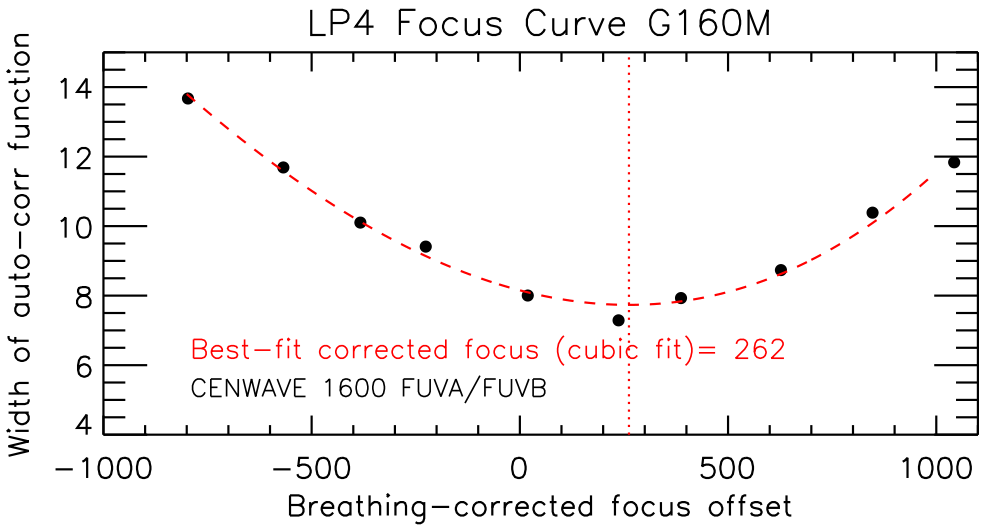

Figure 3. Focus curve for the G160M/1600 setting. The width of the ACF is plotted against breathing-corrected focus offset relative to LP3. Our adopted best-fit focus offset (+262) is the minimum of the cubic fit shown with the red dashed curve.

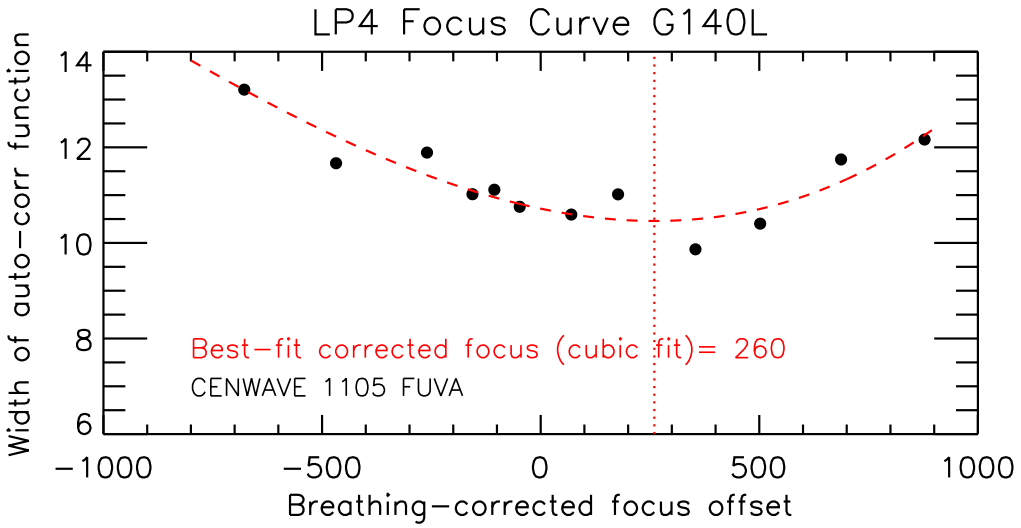

Figure 4. Focus curve for the G140L/1105 setting (FUVA channel only), which is asymmetric with a shallow minimum. The offsets are expressed relative to LP3.

Table 4. History of COS/FUV focus updates since installation. All numbers given are absolute focus values except the final column, which shows the LP3 to LP4 relative offset determined from this analysis and from Sonnentrucker et al. (2017).
[a] Values in the launch version of FSW (build CS4.09a), given in PR 62865.
[b] G130M/1222 focus values for 2nd SMOV update and LP2 are based on models, not measurements.
[c] G140L/1105 value at LP1 was later refined to −656 (Oliveira et al. 2013) and has now been updated (in 2017) in the flight software.

Setting	Launch Focus[a]	1st SMOV Update	2nd SMOV Update	LP2	LP3	LP4	Offset LP4-LP3
G130M/1309	+320	+470	+170	+290	+352	+392	+40
G130M/1222	...	...	–850[b]	–810[b]	–1021	–860	+142
G160M/1600	+6	+156	–44	+116	–30	+232	$+262^{+28}_{-31}$
G140L/1105	–620	–470	–370[c]	–535	–673	–413	$+260^{+98}_{-183}$

5. Results and Conclusions

The focus offsets determined in this ISR are summarized in Table 4, together with all COS/FUV focus values in place since the instrument was installed in 2009. This includes the focus values for G130M/1209 and G130M/1222 recently determined at LP4 by Sonnentrucker et al. (2017). The focus offsets determined from our analysis are listed in the final column. They were patched into the flight software in February 2017 in version LV58, and will be installed on May 2017 in LV59.

Our focus measurements at LP4 can be compared to the expectations from the ray-trace (RT) models shown in Figure 1. The uncertainties in the derived focus position and in the RT models themselves need to be factored into the analysis. A Monte Carlo analysis based on simulated focus curves at LP3 showed that the uncertainty in deriving a G160M/1600 focus offset from a cubic function is $^{+28}_{-31}$ (90% confidence limit; Fox et al. 2015); for G140L/1105 the uncertainty in the focus offset is $^{+98}_{-183}$ (90% c.l.). These errors should approximately hold at LP4, since the shape of the focus curves are similar for both G160M and G140L at both lifetime positions.

For G160M/1600 the derived focus offset of $+262^{+28}_{-31}$ differs from the RT predicted focus offset of +120±50 by +142 steps, or 2.5σ when combining the errors in quadrature (i.e. combining the error in the derived offset with the error in the predicted offset). For G140L/1105 the derived focus offset of $+260^{+98}_{-183}$ differs from the RT prediction of +120±50 by +140 steps, or 0.7σ when combining the errors in a similar way. The 2.5σ difference between the derived and expected focus for G160M/1600 is somewhat larger than expected, but in the final analysis, we rely on the data more than the model, and *both* the ACF technique (Figure 3) and the by-eye inspection of the data (Figure 5) support the adopted G160M/1600 offset of +262 steps. Since there are currently no plans to move the COS/FUV spectrum more than 5.0 arcsec off axis (i.e., further from LP1 than LP4), our results demonstrate that the COS FUV channel can

be successfully focused at all locations on the detector. This bodes well for any future lifetime moves that may be necessary.

Acknowledgments

The authors acknowledge the use of the HST Focus Model tool provided by Colin Cox.

References

Fox, A., et al. 2015, Instrument Science Report COS 2015-01, "The COS/FUV Focus Sweep Program at Lifetime Position 3 (LENA2/13635)"
Ghavamian, P. et al., 2012, Instrument Science Report COS 2012-01, "COS FUV Focus Determination for the G140L Grating"
Lennon, D., et al. 2010, Instrument Science Report COS 2010-07, "SMOV: COS FUV Focus Determination"
Oliveira, C., et al. 2013, Instrument Science Report COS 2013-01, "Second COS FUV Lifetime Position Results from the Focus Sweep Enabling Program, FENA3 (12796)"
Sonnentrucker, P., et al. 2017, Instrument Science Report COS 2017-XX, "FUV Focus Sweep Exploratory Program for COS at LP4"

Appendix

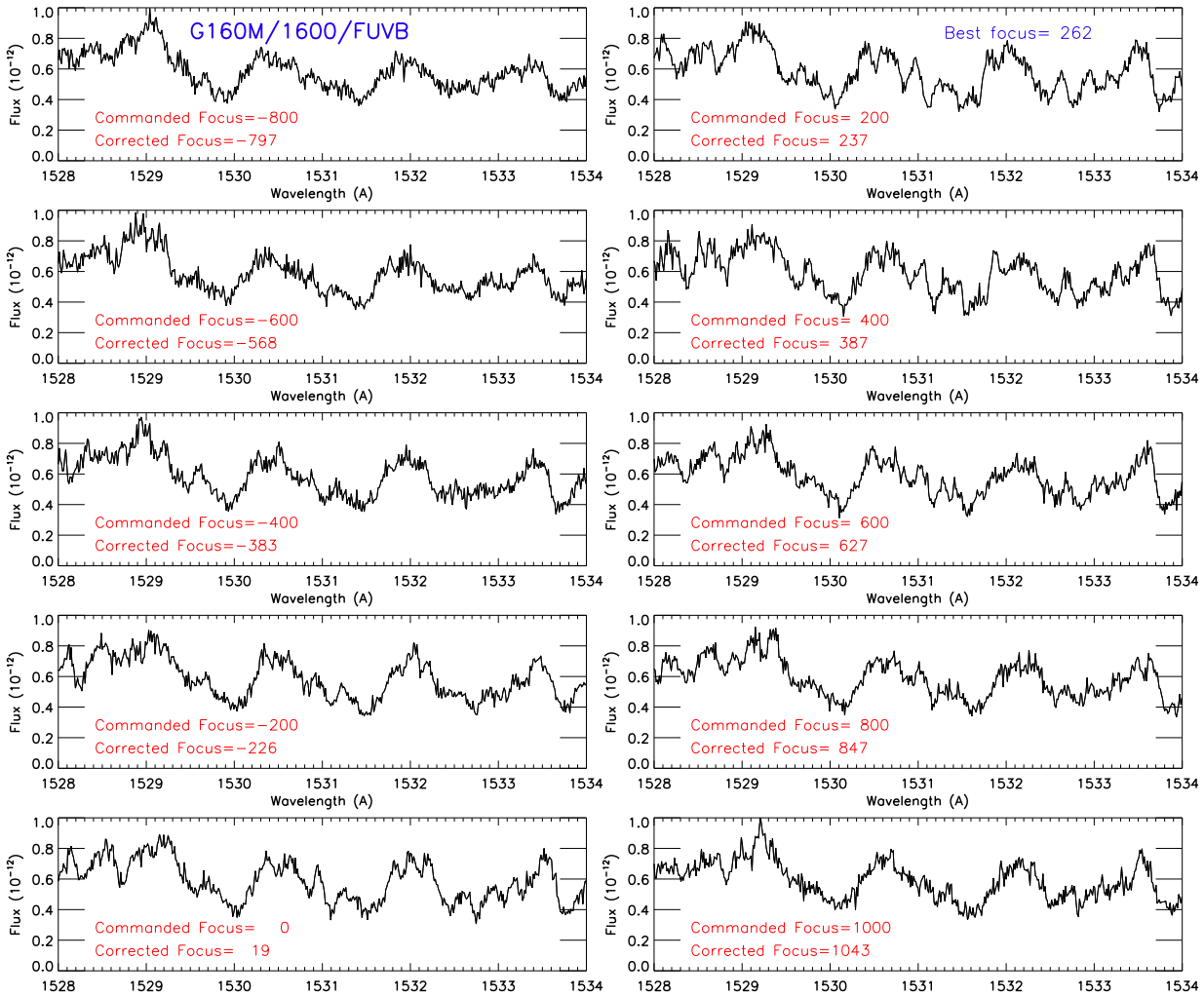

Figure 5. Strong photospheric absorption lines observed in COS FUV spectra of the star Feige 48 in the G160M/1600/FUVB setting. The ten panels show the spectra obtained at each position in the focus sweep (with commanded- and breathing-corrected focus offsets annotated in red). The fluxes are in units of erg s^{-1} cm^{-2} $Å^{-1}$. The best-fit focus for this setting determined from our auto-correlation analysis (+262) is annotated on the panel (at top right) with the closest-matching corrected focus (+237). This panel can be seen by eye to show sharply focused absorption lines, although the preceding and following panels are also useful for this.

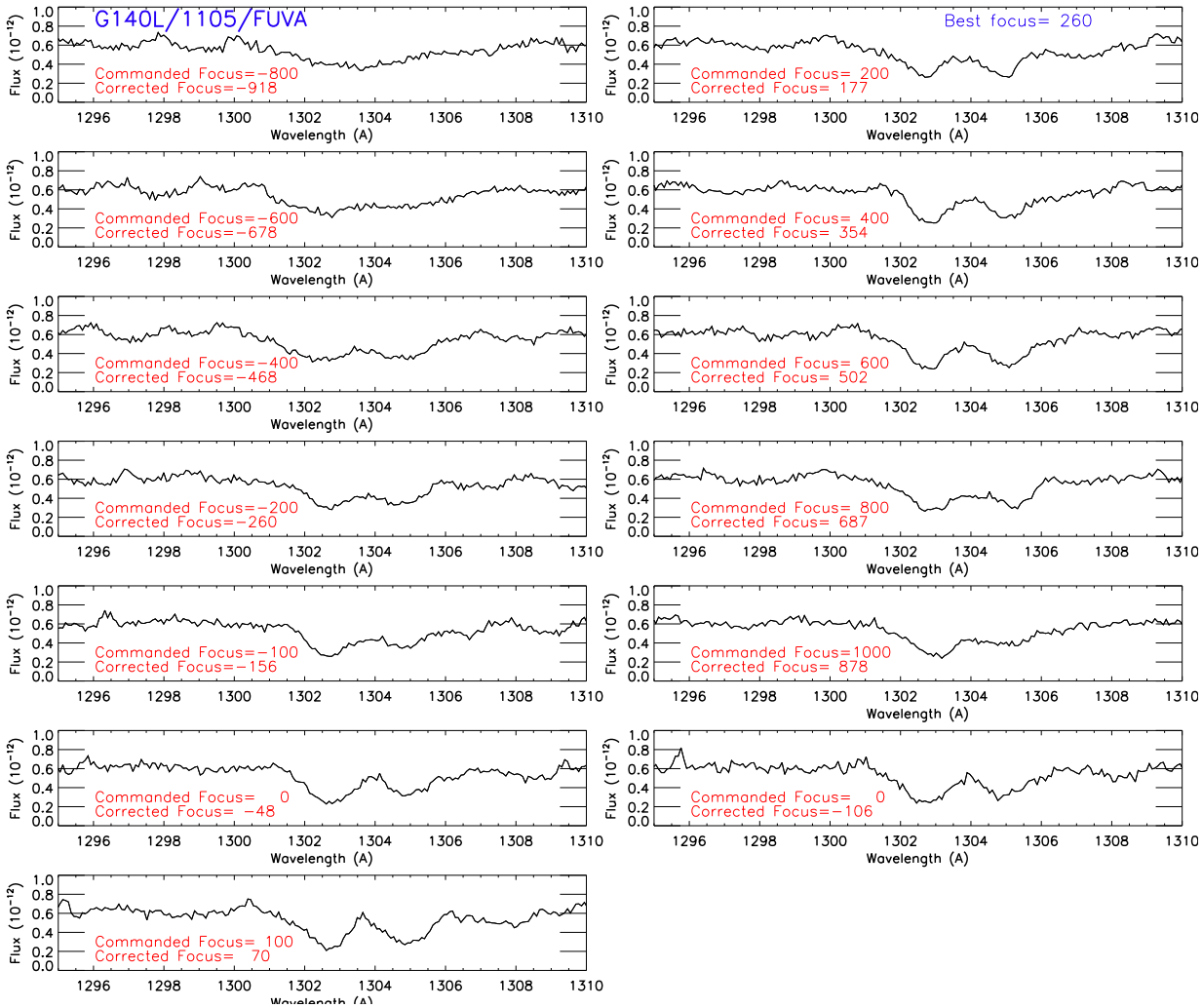

Figure 6. Interstellar absorption lines observed in the G140L/1105/FUVA setting. See Figure 5 for description. These spectra show the target AzV75. The best fit focus found by the ACF technique (+260) is marked on the panel with the closest matching corrected focus.